J. Fluid Mech. (1975), *vol.* 70, *part* 3, *pp.* 481–507
Printed in Great Britain

Inviscid interpenetration of two streams with unequal total pressures

By M. E. GOLDSTEIN
AND WILLIS H. BRAUN

National Aeronautics and Space Administration, Lewis Research Center,
Cleveland, Ohio 44135

(Received 16 September 1974 and in revised form 27 December 1974)

A theory is developed for analysing the inviscid interpenetration of two streams. It is assumed that the difference in total pressure between the streams is not large. Several examples of the general results are presented.

1. Introduction

The fluid mechanics of the interpenetration of moving streams are by no means fully understood. Some insight into this phenomenon can be gained by considering two-dimensional inviscid incompressible flows since such flows are frequently simple enough to be amenable to mathematical analysis. But relatively few analyses of this type have actually been performed. This is due, at least partially, to the fact that they often involve the solution of nonlinear problems in which the shapes of the boundaries are unknown. Fortunately, the classical theory of inviscid flows can be used to obtain solutions for the special case where the total pressures of the streams are equal. Such flows were discussed by Ehrich (1953) and by Woods (1956).

There is another limiting case, called the 'strong jet approximation', in which the analysis can be considerably simplified. This is the case where the total pressure in the injected stream is very much larger than that in the mainstream.† An analysis of this type of jet was first carried out by Taylor (1954), who obtained an analytical solution by introducing an additional approximation. This approximation was removed by Ackerberg & Pal (1968), who used a variational principle to obtain numerical solutions.

In this paper we shall analyse the opposite limit, wherein the difference in total pressure between the two streams is relatively small. We consider a stream discharging from a nozzle or reservoir into a partially moving and partially stationary environment in such a way that where the two streams first interact the flows leave the solid boundaries in a tangential direction (figure 1).‡ A stagnation region with an accompanying free streamline may or may not be present. The flow will be assumed to be two-dimensional, inviscid and incompressible.

† A linearized version of the strong jet approximation was used by Spence (1956) to analyse the jet flap.

‡ This condition serves to eliminate stagnation points where the streamline slope can change discontinuously as the difference in total pressure between the streams becomes non-zero.

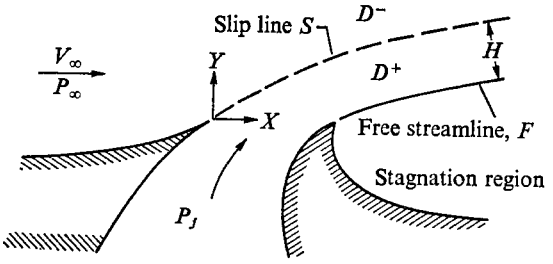

FIGURE 1. Interpenetrating streams.

The velocity will, in general, not be continuous across the streamline or streamlines (denoted by S in figure 1) separating the two streams.

The problem is solved by expanding in a small parameter which is related to the difference in total pressure between the streams.† The zeroth-order solution corresponds to equal total pressures and can be obtained by classical methods such as the Helmholtz–Kirchhoff technique. Since the boundary shapes for the first-order (different total pressures) problem are unknown, a technique similar to that employed in thin-airfoil theory is used to transfer the first-order boundary conditions to the zeroth-order boundary. The transformed problem still involves a combination of boundary and jump conditions which cannot be handled by ordinary techniques. In order to overcome this difficulty we develop a procedure which transforms the problem into one which can be solved by standard techniques of the theory of sectionally analytic functions.‡ This procedure consists of introducing a new dependent variable which satisfies only jump and symmetry conditions on the boundaries rather than the combination of jump and boundary conditions which is imposed on the physical variables.

The general problem is formulated in §2 and the asymptotic expansions are performed in §3. The zeroth- and first-order boundary conditions are deduced in §§4 and 5, respectively. Solutions are then developed for flows both with and (§6) and without (§7) free streamlines. In §8 the general theory is applied to several specific flow configurations.

Although it is assumed herein that the interacting streams are of equal density, the theory can easily be generalized to include streams of unequal (but constant) density (Goldstein & Braun 1969*a*).

2. Formulation and boundary conditions

It will be assumed that the flow is inviscid, incompressible and irrotational. A typical flow configuration is illustrated in figure 1. The analysis is limited to the case in which the difference between the total pressure P_j in the

† The discontinuous change in stream slope which would occur if the tangency condition were not imposed at the confluence of the streams would cause this expansion to become non-uniformly valid at this point and it would then be necessary to use the method of matched asymptotic expansions to complete the solution.

‡ A sectionally analytic function is one which is analytic in the entire complex plane except on a given curve across which its value changes discontinuously (jumps) (Muskhelishvili 1953, § 15).

stream† emanating from the nozzle or reservoir and the total pressure P_∞ in the mainstream is not too large; or more specifically, to the case in which

$$|P_j - P_\infty|/\tfrac{1}{2}\rho V_\infty^2 \equiv |\epsilon| \ll 1, \tag{1}$$

where ρ is the density of the fluid and V_∞ is the velocity of the mainstream at infinity. We let L denote a convenient reference length, which will be specified in the course of the analysis. All lengths are made dimensionless using L (i.e. $x = X/L$, $y = Y/L$ and $h = H/L$) and the complex variable z is defined by $z = x + iy$. The quantities u and v denote the x and y components of the velocity non-dimensionalized by V_∞ and the dimensionless complex-conjugate velocity ζ is defined, as usual, by $\zeta = u - iv$.

The stream of fluid issuing from the nozzle (reservoir) meets the mainstream and forms a common streamline which is denoted by S. Points on this streamline will be denoted by $z^S = x^S + iy^S$. In order to satisfy the requirement that there be no discontinuities in the static pressure $p(x, y)$ anywhere within the flow field, it is necessary (as will be shown subsequently) to allow the velocity to be discontinuous across S. For this reason the streamline S will be called the slip line. The region occupied by the injected stream is denoted by D^+ and the remaining region of the flow (i.e. the mainstream) by D^-. Since the velocity is discontinuous across S, it is convenient to use the superscripts $\pm$ to distinguish between these regions. Thus,

$$\zeta(z) = \zeta^\pm(z), \quad z \in D^\pm.$$

Then ζ^+ is holomorphic in the interior of D^+ and ζ^- is holomorphic in the interior of D^-.

The following argument will show that the velocity must be discontinuous across S. Bernoulli's equation, when applied to the flow within the injected stream, shows that

$$p(x, y)/\tfrac{1}{2}\rho V_\infty^2 + |\zeta^+(z)|^2 = P_j/\tfrac{1}{2}\rho V_\infty^2, \quad z \in D^+, \tag{2}$$

and when applied to the flow external to the jet, that

$$p(x, y)/\tfrac{1}{2}\rho V_\infty^2 + |\zeta^-(z)|^2 = P_\infty/\tfrac{1}{2}\rho V_\infty^2, \quad z \in D^-. \tag{3}$$

But, since S is a common streamline of the external and internal flow, and since the static pressure cannot be discontinuous across this line, it follows from (2) and (3) that

$$|\zeta^+(z^S)|^2 - |\zeta^-(z^S)|^2 = (P_j - P_\infty)/\tfrac{1}{2}\rho V_\infty^2 = \epsilon \tag{4}$$

at every point z^S of S.

It is convenient in the analysis which follows to replace the complex-conjugate velocity ζ by the variable Ω, which is related to it by

$$\zeta^\pm = \exp \Omega^\pm. \tag{5}$$

Then the 'jump' condition (4) becomes

$$|\exp \Omega^+|^2 - |\exp \Omega^-|^2 = \epsilon \quad \text{for} \quad z \in S. \tag{6}$$

Moreover, since the velocities inside and outside the jet must have a common direction at each point of S, it follows that

$$\operatorname{Im} \Omega^+ = \operatorname{Im} \Omega^- \quad \text{for} \quad z \in S. \tag{7}$$

† Which is assumed for definiteness to be of finite width at downstream infinity.

Since there is no flow in the stagnation region (if such a region is present), it is clear that the static pressure along the free streamline F is constant and equal to the pressure in this region. Furthermore, very far downstream the velocities of the mainstream and injected stream become uniform, and as a consequence the pressure in the stagnation region must be equal to the pressure p_∞ of the mainstream at infinity. Hence, (2) and (5) show that for any point on F

$$|\exp\Omega^+|^2 = \frac{P_j - p_\infty}{\frac{1}{2}\rho V_\infty^2} = 1 + \frac{P_j - (p_\infty + \frac{1}{2}\rho V_\infty^2)}{\frac{1}{2}\rho V_\infty^2} = 1 + \frac{P_j - P_\infty}{\frac{1}{2}\rho V_\infty^2} = 1 + \epsilon, \quad z \in F. \tag{8}$$

We can ensure that F will be a streamline by setting the cross-product of the velocity and a differential of arc equal to zero to obtain

$$\operatorname{Im}\{\exp[\Omega^+(z^F)]\, dz^F\} = 0. \tag{9}$$

The conditions imposed on the velocity at infinity are

$$\exp[\Omega^+(z)] \to \text{constant} \quad \text{as} \quad z \to \infty \quad \text{in the reservoir or nozzle} \tag{10}$$

and

$$\Omega^-(z) \to 0 \quad \text{as} \quad z \to \infty \quad \text{in the mainstream.} \tag{11}$$

On solid boundaries the slope of the velocity $\bar{\zeta}^\pm$ equals the slope m of the wall, so that

$$\operatorname{Im}\Omega^\pm(z) = -\tan^{-1} m(z) \quad \text{for } z \text{ on a solid boundary.} \tag{12}$$

These conditions are sufficient to determine the solution completely, provided it exists.†

3. Asymptotic expansions

We assume that the functions $\Omega^\pm$ can be expanded in asymptotic power series in ϵ. Then, in view of the fact that the shapes of the slip line and of the free streamline depend on ϵ, these expansions imply that the co-ordinates z^S and z^F of S and F, respectively, and the asymptotic width h of the injected stream also possess such expansions. Hence

$$\left.\begin{aligned} \Omega^\pm &= \Omega_0 + \epsilon\Omega_1^\pm \ldots, \quad z^S = z_0^S + \epsilon z_1^S + \ldots, \\ z^F &= z_0^F + \epsilon z_1^F + \ldots, \quad h = h_0 + \epsilon h_1 + \ldots. \end{aligned}\right\} \tag{13}$$

The reason for omitting the superscripts $\pm$ on the zeroth-order terms of the expansions for $\Omega^\pm$ is that the continuity of these terms across S (which we shall establish subsequently) ensures that there will be a single function Ω_0 which is holomorphic in the entire flow field.

The reference length L will now be chosen to make $h_0 = 1$, which means that L is the zeroth-order asymptotic thickness of the injected stream. This is denoted symbolically by putting

$$L = H_0. \tag{14}$$

The last expansion in (13) is then

$$h = 1 + \epsilon h_1 + \ldots. \tag{15}$$

† A reviewer has pointed out that the boundary-value problems for certain containing flows do not always possess solutions.

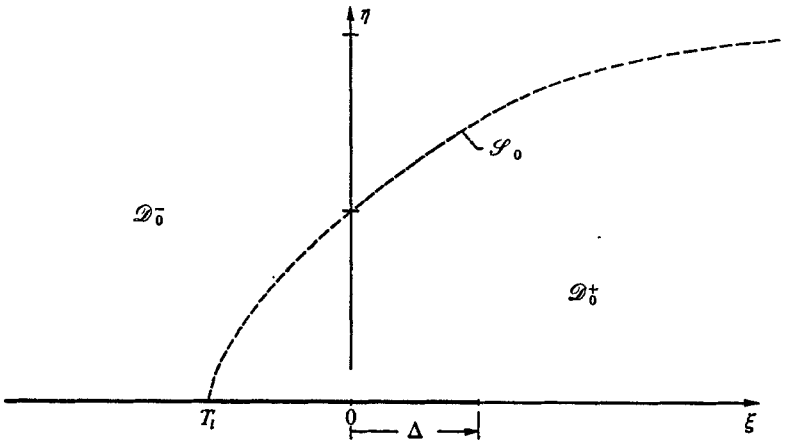

FIGURE 2. Intermediate (T) plane.

4. Zeroth-order solution

When the expansions (13) are substituted into the boundary conditions (6)–(12) and only the zeroth-order terms are retained, the following boundary conditions for the zeroth-order solution are obtained. First, boundary conditions (6) and (7) show (as has already been anticipated) that the zeroth-order solution must be continuous across the slip line and hence that it is characterized by a function which is holomorphic everywhere within the flow field. The remaining conditions show that

$$|\zeta_0(z_0^F)| = 1, \quad \mathrm{Im}\{\zeta_0(z_0^F)\, dz_0^F\} = 0, \tag{16 a, b}$$

$$\mathrm{Im}\,\Omega_0(z) = -\tan^{-1} m(z) \quad \text{for } z \text{ on solid boundaries}, \tag{16 c}$$

$$\zeta_0(z) = \text{constant} \quad \text{as } z \to \infty \text{ in the reservoir or nozzle}, \tag{16 d}$$

$$\Omega_0(z) = 0 \quad \text{as } z \to \infty \text{ in the mainstream}, \tag{16 e}$$

where we have put $\zeta_0(z) \equiv \exp[\Omega_0(z)]$.

Now the boundary-value problem posed by the boundary conditions (16), whether or not it involves a free streamline, can in principle be solved by classical methods such as the Helmholtz–Kirchhoff technique (see, for example, Birkhoff & Zarantonello 1957, chap. V). This is often accomplished by mapping the hodograph plane and the complex potential plane into the upper half of an intermediate T plane in such a way that the free streamlines and solid boundaries map onto the real axis (figure 2). We shall denote the real and imaginary parts of the variable T by ξ and η, respectively. We let $\mathscr{D}_0^+$ denote the region of the T plane into which the zeroth-order injected stream maps and $\mathscr{D}_0^-$ denote the region of the T plane into which the zeroth-order mainstream maps. The dividing line between these two regions (which is called for convenience the zeroth-order slip line even though no slip occurs in the zeroth-order solution) is denoted by $\mathscr{S}_0$.

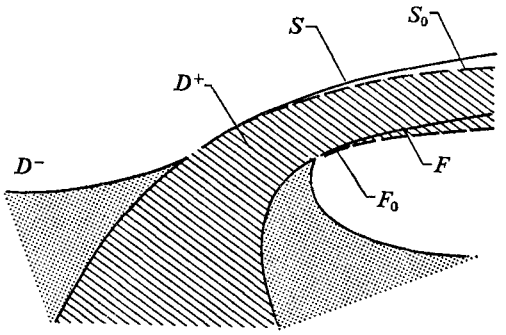

FIGURE 3. Comparison of zeroth-order and true boundaries in the physical plane.

5. Formulation of first-order problem in physical plane

The mapping $T \to z$ introduced in the preceding section transforms the upper half T plane approximately into the region of flow in the physical plane. The domain $\mathscr{D}_0^+$ is mapped into the cross-hatched region shown in figure 3. The curve $\mathscr{S}_0$ and the line segment EC are mapped into the dashed boundaries S_0 and F_0, respectively. This region, of course, differs from the true interior of the jet, whose boundaries S and F are indicated by the solid lines in the figure.

The boundary conditions (6)–(9) are specified on the curves S and F. Although the shapes of these curves are not known at this stage of the solution, they can differ from those of S_0 and F_0 (which are known) by quantities which are at most of order ϵ. Since, as far as the first-order solution is concerned, the boundary conditions only have to be satisfied up to and including terms of order ϵ, we shall attempt to transfer the boundary conditions correct to terms of order ϵ from S and F to S_0 and F_0, respectively. To this end recall that the solution has been divided into two parts (indicated by the superscripts $\pm$), one of which is holomorphic in D^+, the other being holomorphic in D^-. We shall assume where necessary (as is done in thin-airfoil theory) that each of these portions of the solution can be analytically continued across S and F to S_0 and F_0, respectively. Thus the values of $\Omega^\pm$ at a point z^S of S can be expressed in terms of their values at the neighbouring point z_0^S of S_0 by performing a Taylor series expansion† about z_0^S. Of course, similar remarks apply to F. Hence

$$\Omega^\pm(z^S) = \Omega^\pm(z_0^S) + (d\Omega^\pm/dz)_{z=z_0^S}(z^S - z_0^S) + \dots,$$
$$\Omega^+(z^F) = \Omega^+(z_0^F) + (d\Omega^+/dz)_{z=z_0^F}(z^F - z_0^F) + \dots.$$

Substituting the asymptotic expansions (13) into these series and retaining terms $O(\epsilon)$ shows that

$$\Omega(z^S) = \Omega_0(z_0^S) + \epsilon[\Omega_1^\pm(z_0^S) + (d\Omega_0/dz)_{z=z_0^S} z_1^S] + O(\epsilon^2), \tag{17}$$

$$\Omega^+(z^F) = \Omega_0(z_0^F) + \epsilon[\Omega_1^+(z_0^F) + (d\Omega_0/dz)_{z=z_0^F} z_1^F] + O(\epsilon^2). \tag{18}$$

By substituting these expressions into the boundary conditions (6)–(9) and neglecting terms $O(\epsilon^2)$ we can find the boundary conditions which the first-order

† That is, $\Omega^\pm$ can, if necessary be analytically continued to z_0^S.

solutions must satisfy on the known boundaries S_0 and F_0. Thus conditions (6) and (7) show that on the slip line

$$\mathrm{Re}\,[\Omega_1^+(z_0^S)-\Omega_1^-(z_0^S)]=2|\zeta_0(z_0^S)|^{-2} \tag{19}$$

and

$$\mathrm{Im}\,\Omega_1^+(z_0^S)=\mathrm{Im}\,\Omega_1^-(z_0^S), \tag{20}$$

while (8) and (9) show that on the free streamline

$$\mathrm{Re}\,[\Omega_1^+(z_0^F)+(d\Omega_0/dz)_{z=z_0^F}z_1^F]=\tfrac{1}{2} \tag{21}$$

and

$$\mathrm{Im}\left\{\zeta_0(z_0^F)\left\{\frac{dz_1^F}{dS_0^F}+\left[\Omega_1^+(z_0^F)+\left(\frac{d\Omega_0}{dz}\right)_{z=z_0^F}z_1^F\right]\frac{dz_0^F}{dS_0^F}\right\}\right\}=0, \tag{22}$$

where d/dS_0^F denotes differentiation with respect to distance along the zeroth-order free streamline. Equations (19)–(22) are the boundary conditions for the first-order solutions 'transferred' from the boundaries S and F to the zeroth-order boundaries S_0 and F_0, and hence the first-order boundary-value problem has been transformed from one in which the shapes of the boundaries are unknown to one in which they are known.

Equations (19) and (20) can be combined to give the following single slip-line boundary condition:

$$\Omega_1^+(z_0^S)-\Omega_1^-(z_0^S)=2|\zeta_0(z_0^S)|^{-2}. \tag{23}$$

The variable z_1^F can be eliminated between conditions (21) and (22) to yield a single boundary condition for Ω_1^+ on F_0. To this end we first note that for any analytic function $G(z)$ and any zeroth-order streamline z_0 on which the length of arc is denoted by S_0

$$\begin{aligned}\frac{dG}{dS_0}&=\frac{dx_0}{dS_0}\left(\frac{\partial G}{\partial x}\right)_{x=x_0}+\frac{dy_0}{dS_0}\left(\frac{\partial G}{\partial y}\right)_{y=y_0}=\left(\frac{dx_0}{dS_0}+i\frac{dy_0}{dS_0}\right)\left(\frac{dG}{dz}\right)_{z=z_0}\\&=\frac{\bar{\zeta}_0(z_0)}{|\zeta_0(z_0)|}\frac{dG(z_0)}{dz_0}=\frac{|\zeta_0(z_0)|}{\zeta_0(z_0)}\frac{dG(z_0)}{dz_0}.\end{aligned} \tag{24}$$

When S_0 is taken to be the zeroth-order free streamline F_0 [characterized by (16 *a*)], this shows that

$$\frac{i}{\zeta_0(z_0^F)}\frac{d\Omega_0}{dz_0^F}=i\frac{d}{dS_0^F}[\ln|\zeta_0(z_0^F)|+i\arg\zeta_0(z_0^F)]=-\frac{d}{dS_0^F}\arg\zeta_0, \tag{25}$$

which is a real quantity. Hence the second term on the left side of (21) becomes

$$\mathrm{Re}\left\{\left(\frac{d\Omega_0}{dz}\right)_{z=z_0^F}z_1^F\right\}=\frac{i}{\zeta_0(z_0^F)}\left(\frac{d\Omega_0}{dz}\right)_{z=z_0^F}\mathrm{Im}\,\{\zeta_0(z_0^F)z_1^F\}, \tag{26}$$

so that (21) implies that

$$\mathrm{Im}\,\{\zeta_0(z_0^F)z_1^F\}=\mathrm{Re}\left\{\frac{\zeta_0(z_0^F)}{i\,(d\Omega_0/dz)_{z=z_0^F}}(\tfrac{1}{2}-\Omega_1^+(z_0^F))\right\}. \tag{27}$$

Upon using (16 *a*) and the relation $\bar{\zeta}_0(z_0^F)=dz_0^F/dS_0^F$ we find that (22) can be rearranged to obtain

$$\frac{d}{dS_0^F}\mathrm{Im}\,[\zeta_0(z_0^F)z_1^F]+\mathrm{Im}\,\Omega_1^+(z_0^F)=0. \tag{28}$$

Combining (27) and (28) now shows that

$$\mathrm{Re}\frac{1}{\zeta_0(z_0^F)}\frac{d}{dz_0^F}\left\{\frac{\zeta_0(z_0^F)}{i(d\Omega_0/dz)_{z=z_0^F}}[\tfrac{1}{2}-\Omega_1^+(z_0^F)]\right\}+\mathrm{Im}\,\Omega_1^+(z_0^F)=0, \tag{29}$$

which becomes, upon differentiating by parts,

$$\mathrm{Im}\frac{d}{dz}\left[(\tfrac{1}{2}-\Omega_1^+)\frac{dz}{d\Omega_0}\right]=0 \quad \text{for } z \text{ on } S_0^F. \tag{30}$$

Finally, combining condition (12) with (16*c*) shows that

$$\mathrm{Im}\,\Omega(z_1^\pm)=0 \quad \text{for } z \text{ on solid boundaries.} \tag{31}$$

6. Flows in which a free streamline is present

6.1. *Solution*

First consider the case where there is a free streamline but the solid boundaries consist only of straight-line segments. Then the zeroth-order problem can always be solved by the Helmholtz–Kirchhoff technique. We shall, for the most part, be able to construct the first-order solution without considering the detailed properties of the zeroth-order solution. However, in order to express this solution in explicit form, it is necessary to know certain features of the asymptotic behaviour of the zeroth-order solution as $T\to\infty$ and $T\to T_l$ (see figure 2). By using the methods given in Birkhoff & Zarantonello (1957, chap. IV) we can show that this behaviour is completely determined by local conditions and will, therefore, be the same for all flows under consideration. Thus, in particular, we can show that

$$z\sim T, \quad dz/d\Omega_0=o(z^2) \quad \text{as} \quad T\to\infty \tag{32}$$

and

$$dz/d\Omega_0=O(T-T_l), \quad z\sim a+bT \quad \text{as} \quad T\to T_l. \tag{33}$$

In order to construct the first-order solution it is convenient first to transform some of the boundary conditions in the physical plane in a certain manner which is suggested by the form of the free-streamline condition (30). To this end notice that (25) shows that $i\zeta_0^{-1}(z)\,d\Omega_0(z)/dz$ is real on these boundaries. Hence the boundary condition (31) on the solid boundaries may be written as

$$\begin{aligned}0&=\mathrm{Im}\frac{1}{|\zeta_0|}\frac{d}{dS_0}\left[\zeta_0\frac{dz}{d\Omega_0}(\Omega_1^\pm+k_1^\pm)\right]\\&=\mathrm{Im}\frac{d}{dz}\left[\frac{dz}{d\Omega_0}(\Omega_1^\pm+k_1^\pm)\right]+\mathrm{Im}\,(\Omega_1^\pm+k_1^\pm)\\&=\mathrm{Im}\frac{d}{dz}\left[\frac{dz}{d\Omega_0}(\Omega_1^\pm+k_1^\pm)\right],\end{aligned} \tag{34}$$

where the $k_1^\pm$ can be any real constants.

The boundary condition (23) along the slip line can also be written in terms of the variable appearing in (30) and (34), by multiplying by $dz/d\Omega_0$ and differentiating along the zeroth-order slip line to obtain

$$\frac{d}{dz}\left\{\frac{dz}{d\Omega_0(z)}[\Omega_1^+(z)-\Omega_1^-(z)]\right\}=\frac{\zeta_0(z_0^S)}{2\,|\zeta_0(z_0^S)|}\frac{d}{dS_0^S}\left\{\frac{dz_0^S}{d\Omega_0(z_0^S)}\frac{1}{|\zeta_0(z_0^S)|^2}\right\} \quad \text{for } z \text{ on } S_0, \tag{35}$$

where S_0^S denotes the distance measured along the slip line. The derivatives on the left may be taken with respect to z because the quantity in the braces is analytic. This is not true for the quantity on the right side.

The boundary conditions (30), (34) and (35) (together with the appropriate conditions at infinity) are just sufficient to determine the analytic functions $\Omega_1^{\pm}$. Since they are specified on the zeroth-order boundaries, they actually determine $\Omega_1^{\pm}$ in the zeroth-order regions of flow. And since these regions are mapped into the upper half T plane by the zeroth-order solution† it is convenient to transform the boundary-value problem into that plane. Then, since $\zeta_0\, dz/dT$ is real on the real T axis (into which the free streamlines and solid boundaries are mapped), the boundary conditions (30)–(35) show that the function

$$\Lambda(T) \equiv \begin{cases} \Lambda^+(T) \equiv \zeta_0 \dfrac{d}{dT}\left[\dfrac{dz}{d\Omega_0}(\Omega_1^+ - \tfrac{1}{2})\right] & \text{for} \quad T \in \mathscr{D}_0^+, \qquad (36a) \\ \Lambda^-(T) \equiv \zeta_0 \dfrac{d}{dT}\left[\dfrac{dz}{d\Omega_0}\Omega_1^-\right] & \text{for} \quad T \in \mathscr{D}_0^-, \qquad (36b) \end{cases}$$

which is sectionally analytic in the upper half T plane cut along the zeroth-order slip line $\mathscr{S}_0$, satisfies the boundary conditions

$$\left.\begin{aligned} \Lambda^+(T) - \Lambda^-(T) &= \Gamma(T) \quad \text{for} \quad T \in \mathscr{S}_0, \\ \operatorname{Im} \Lambda(\xi + i0) &= 0 \quad \text{for} \quad -\infty < \xi < +\infty, \end{aligned}\right\} \qquad (37)$$

where we have put‡

$$\Gamma(T) = \frac{1}{2}\frac{\zeta_0^2(T)}{|\zeta_0(T)|}\frac{dz(T)}{dT}\frac{d}{dS_0^S}\left[\frac{dz}{d\Omega_0}\left(\frac{1}{|\zeta_0(T)|^2} - 1\right)\right] \quad \text{for} \quad T \in \mathscr{S}_0. \qquad (38)$$

Now suppose that Θ is a sectionally analytic function which satisfies conditions (37). Then, if ω is any function which is analytic in the interior of the upper half-plane and which is real on the real axis, the function $\Theta + \omega$ also satisfies the boundary conditions (37). First, suppose that ω has no singularities on the real axis. Then the Schwartz reflexion principle shows that ω has an analytic continuation to the entire T plane and therefore has a Taylor series expansion about the origin which has real coefficients. Thus ω can be represented in the form

$$\sum_{n=0}^{N} c_n T^n \text{ with } c_n \text{ real.}$$

If $N = +\infty$, ω has an essential singularity at $T = +\infty$; if N is finite, ω has a pole of order N at $T = +\infty$. It will be shown subsequently that the behaviour of ζ at $T = \infty$ dictates that N be finite. On the other hand if ω does have singularities on the real axis, the requirement that ω be real there shows that they cannot be branch points. Hence these singularities must be poles or perhaps essential singularities. However, an investigation of the solutions shows that, if ζ is to be bounded, the only singularity which can be allowed is a simple pole at the origin.

† Then the function $z = z(T)$, which is the inverse of this mapping, is given by the zeroth-order solution.

‡ The notation $\Gamma(T)$ is not meant to indicate that Γ is an holomorphic (analytic) function of T. In fact Γ is defined only on $\mathscr{S}_0$.

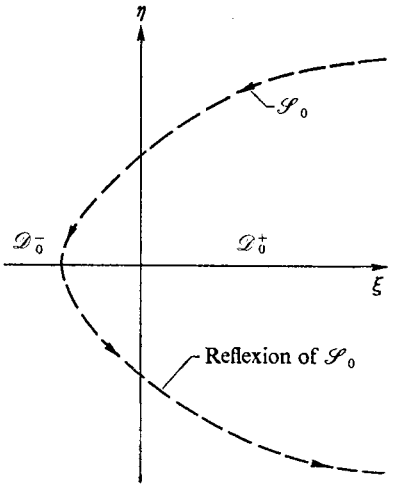

FIGURE 4. Path of integration in the T plane.

Upon using the fact that† $\zeta_0 dz/dT$ is real on the real T axis we see that the solution to the boundary-value problem (37) can be expressed as

$$\Lambda(T) = \Theta(T) + \sum_{n=0}^{N} c_n T^n + \alpha\zeta_0(T)\frac{dz}{dT} \quad \text{for} \quad \mathrm{Re}\, T > 0, \tag{39}$$

where c_n and α are real constants and Θ is a sectionally analytic function which vanishes at infinity, is bounded on the real axis and is a solution of the boundary-value problem (37).

We shall first construct the function Θ. To this end let the reflexion of the curve $\mathscr{S}_0$ in the real axis be designated by $\mathscr{S}_0'$ (figure 4). The function $\Gamma(T)$, defined on $\mathscr{S}_0$ in the upper half-plane, can be extended to $\mathscr{S}_0'$ by setting

$$\Gamma(T) = \overline{\Gamma(\overline{T})} \quad \text{for} \quad T \in \mathscr{S}_0'. \tag{40}$$

It follows from conditions (32) and (33) that $\Gamma(T)$ vanishes like some power (perhaps fractional) of T as $T \to \infty$ and remains finite at the intersection of $\mathscr{S}_0$ with the real axis. It can also be shown that this intersection occurs at right angles to the real axis. Then the Plemelj formulae (Muskhelishvili 1953, p. 42) show that the Cauchy integral

$$\Theta = \frac{1}{2\pi i}\int_{\mathscr{S}_0+\mathscr{S}_0'} \frac{\Gamma(\tau)}{\tau - T}\, d\tau \tag{41}$$

(where the integration is to be performed in the counterclockwise (positive) direction along $\mathscr{S}_0$ and $\mathscr{S}_0'$) is indeed a sectionally analytic function which is real (and bounded) on the real axis, satisfies the jump condition in (37) and vanishes at infinity. In fact, they show that

$$\Theta^{\pm}(T) = \pm\tfrac{1}{2}\Gamma(T) + \frac{1}{2\pi i}\mathrm{P}\int_{\mathscr{S}_0+\mathscr{S}_0'} \frac{\Gamma(\tau)}{\tau - T}\, d\tau \quad \text{for} \quad T \in \mathscr{S}_0 + \mathscr{S}_0', \tag{42}$$

where P denotes the Cauchy principal value and the convention for the $\pm$ superscript is that used previously.

† Recall that the function $z(T)$ is determined by the zeroth-order solution.

The definition (36 *a*), when combined with (39), shows that for $T \in \mathscr{D}_0^+$

$$\zeta_0(T)\frac{d}{dT}\left[\frac{dz}{d\Omega_0}(\Omega_1^+(T)-\tfrac{1}{2})\right] = \Theta(T) + \sum_{n=0}^{N} c_n T^n + \alpha\zeta_0\frac{dz}{dT}, \tag{43}$$

or, after integration, that

$$\Omega_1^+(T) = \tfrac{1}{2} + \frac{d\Omega_0(T)}{dz(T)}\left[\int_{T_l}^{T}\frac{\Theta(T)\,dT}{\zeta_0(T)} + \sum_{n=0}^{N} c_n \int_{T_l}^{T}\frac{T^n dT}{\zeta_0(T)} + \alpha z(T) + \beta\right]. \tag{44}$$

But using the estimates (32) and (33) and the fact that $\Theta(T) = o(1)$ as $T \to \infty$ (Gakhov 1966, § 4.6) we find that the constants β and c_n ($n \neq 0$) must vanish if the function $\Omega_1^+(T)$ is to be bounded. Hence the first-order solution is given by

$$\Omega_1^+(T) = \tfrac{1}{2} + \frac{d\Omega_0}{dz}\left[\int_{T_l}^{T}\frac{\Theta(T)+c_0}{\zeta_0(T)}dT + \alpha z(T)\right], \tag{45}$$

with Θ determined by (38) and (41).

The constants α and c_0 can easily be determined in any specific problem by requiring that $\Omega_1^+(T)$ remain bounded and that no new fluid be added to the injected flow (continuity). A similar expression can easily be obtained for Ω_1^-. In order to complete the solution it is necessary to calculate the positions of the slip line and the free streamline.

6.2. *Derivation of boundary values*

Multiplying (45) by $\zeta_0\,dz/dT$ and integrating by parts shows that

$$\begin{aligned}\int_{z_0^i}^{z}\zeta_0(\Omega_1^+-\tfrac{1}{2})\,dz &= \int_{T_i}^{T}\zeta_0(\Omega_1^+-\tfrac{1}{2})\frac{dz}{dT}dT \\ &= \zeta_0(T)\int_{T_i}^{T}\frac{\Theta+c_0}{\zeta_0}dT - \int_{T_l}^{T}(\Theta+c_0)\,dT - \alpha\int_{T_i}^{T}\zeta_0\frac{dz}{dT}dT \\ &\quad + \left[\int_{T_l}^{T_i}\frac{\Theta+c_0}{\zeta_0}dT\right][\zeta_0(T)-\zeta_0(T_i)] + \alpha[z(T)\,\zeta_0(T) - z(T_i)\,\zeta_0(T_i)],\end{aligned} \tag{46}$$

where T_i is the image in the T plane of the initial point z_0^i. Using (46) in equation (A 4) (see appendix) with $f(\mathscr{S}_0)$ taken equal to $\frac{1}{2}-\alpha$ shows that the position $z^{\mathscr{S}}$ of any streamline $\mathscr{S}$ is determined by†

$$\begin{aligned}z^{\mathscr{S}} = z(T) - \epsilon\Bigg\{&\int_{T_i}^{T}\frac{\Theta+c_0}{\zeta_0}dT - \frac{1}{\zeta_0}\int_{T_i}^{T}(\Theta+c_0)\,dT \\ &+ \left[\int_{T_l}^{T_i}\frac{\Theta+c_0}{\zeta_0}dT\right]\left[1-\frac{\zeta_0(T_i)}{\zeta_0(T)}\right] + \alpha\left[z(T) - \frac{\zeta_0(T_i)}{\zeta_0(T)}z(T_i)\right]\Bigg\} \quad \text{for} \quad T \in \mathscr{S}_0.\end{aligned} \tag{47}$$

The two bounding streamlines are the slip line and the free streamline. The initial point T_i on the slip line is T_l as may be verified by reference to figure 2. Then putting $T_i = T_l$ (46) with $z(T_l) = 0$ (as indicated in figure 1) shows that

$$z^S = z(T)[1-\epsilon\alpha] - \epsilon\left[\int_{T_i}^{T}\frac{\Theta+c_0}{\zeta_0}dT - \frac{1}{\zeta_0(T)}\int_{T_l}^{T}(\Theta+c_0)\,dT\right] \quad \text{for} \quad T \in \mathscr{S}_0. \tag{48}$$

† $z(T)$ with $T \in \mathscr{S}_0$ gives the location in the physical plane of the zeroth-order streamline $\mathscr{S}_0$.

The zeroth-order free streamline maps into the real T axis. We can suppose without loss of generality that it occupies the region $\xi > \Delta$ for some constant $\Delta > 0$. Then

$$z^F = z(\Delta) + [z(T) - z(\Delta)](1 - \epsilon\alpha) - \epsilon\left\{\int_\Delta^T \frac{\Theta + c_0}{\zeta_0} dT - \frac{1}{\zeta_0(T)}\int_\Delta^T (\Theta + c_0)\, dT \right.$$
$$\left. + \left[\alpha z(\Delta) + \int_{T_l}^\Delta \frac{\Theta + c_0}{\zeta_0} dT\right]\left[1 - \frac{\zeta_0(\Delta)}{\zeta_0(T)}\right]\right\} \quad \text{for} \quad T = \xi + i0, \quad \xi > \Delta. \tag{49}$$

It follows from (5), (13), (17), (45) and (48) that the velocity of the injected flow at the slip line is given by

$$\zeta^+(T) = \zeta_0(T)\left\{1 + \frac{\epsilon}{2} + \frac{\epsilon}{\zeta_0(T)} \frac{d\Omega_0(T)}{dz(T)} \int_{T_l}^T (\Theta + c_0)\, dT\right\} \quad \text{for} \quad T \in \mathscr{S}_0, \tag{50}$$

which shows that the slip-line pressure coefficient, defined by

$$C_{pS} \equiv [p_0 - p(x_S, y_S)]/\tfrac{1}{2}\rho V_\infty^2 = |\zeta^+(z^S)|^2,$$

is given by

$$C_{pS} = |\zeta_0(T)|^2\left\{1 + \epsilon + 2\epsilon\,\mathrm{Re}\left[\frac{1}{\zeta_0(T)} \frac{d\Omega_0(T)}{dz(T)} \int_{T_l}^T (\Theta + c_0)\, dT\right]\right\} \quad \text{for} \quad T \in \mathscr{S}_0. \tag{51}$$

The distance $\hat{S}$ measured along the slip line S is

$$\hat{S} = H_0 \int_{T_l}^T \left|\frac{dz^S}{dT}\right| |dT| \quad \text{for} \quad T \in \mathscr{S}_0. \tag{52}$$

But by using (48) and (50) and recognizing that $1 - \zeta^+/\zeta_0$ is $O(\epsilon)$, it can be shown that

$$\frac{dz^S}{dT} = \frac{dz_0^S}{dT} \frac{\zeta_0}{\zeta^+}[1 + \epsilon(\tfrac{1}{2} - \alpha)] + O(\epsilon^2).$$

Hence

$$\frac{\hat{S}}{H_0} = [1 + \epsilon(\tfrac{1}{2} - \alpha)] \int_{T_l}^T \left|\frac{dz_0^S}{dT}\right| \left|\frac{\zeta_0(z_0^S)}{\zeta^+(z_0^S)}\right| |dT| \quad \text{for} \quad T \in \mathscr{S}_0. \tag{53}$$

7. Flows with no free streamline

7.1. *Solution*

When the flow has no free streamlines, the injected flow is bounded only by slip lines and solid boundaries. The boundary conditions are, therefore, given by (23) and (31). In this case it is no longer necessary to require the solid boundaries to be straight-line segments. In order to find a representation of the flow in terms of a Cauchy integral we now define a sectionally analytic function $\Theta(T)$ in the T plane by

$$\Theta(T) = \begin{cases} \Theta^+(T) = \Omega_1^+(T) - \tfrac{1}{2} & \text{for} \quad T \in \mathscr{D}_0^+, \\ \Theta^-(T) = \Omega_1^-(T) & \text{for} \quad T \in \mathscr{D}_0^-. \end{cases} \tag{54}$$

Then on the transformed slip line(s) $\mathscr{S}_0$ the boundary condition is

$$\Theta^+(T) - \Theta^-(T) = \Gamma(T) \quad \text{for} \quad T \in \mathscr{S}_0,$$

where now

$$\Gamma(T) \equiv \tfrac{1}{2}[|\zeta_0(T)|^{-2} - 1]. \tag{55}$$

Moreover, since the real axis is now the image of the solid boundaries it follows from (12) and (16) that

$$\operatorname{Im}\Theta^+(T) = 0 \quad \text{for} \quad \operatorname{Im} T = 0.$$

Again, let $\Gamma(T)$ be continued into the lower half-plane according to (40) and define the reflexion of $\mathscr{S}_0$ in the real axis to be $\mathscr{S}_0'$. Then the solution $\Theta(T)$ (which is everywhere bounded) is simply given by (41).

7.2. *Derivation of boundary values*

The position of the slip line is obtained by substituting (54) into (A 4) with $f(\delta_0)$ set equal to $\frac{1}{2}$:

$$z^S(T) = z(T) - \frac{\epsilon}{\zeta_0(T)} \int_{T_l}^{T} \Theta^+(T)\,\zeta_0(T) \frac{dz_0^S}{dT}\,dT \quad \text{for} \quad T \in \mathscr{S}_0. \tag{56}$$

Combination of (5), (17), (54) and (56) shows that the pressure coefficient along the slip line is

$$C_{pS} = |\zeta^+(z^S)|^2 = |\zeta_0(T)|^2 \times \left\{1 + \epsilon + 2\epsilon \operatorname{Re}\left[\Theta^+(T) - \frac{1}{\zeta_0(T)} \frac{d\Omega_0}{dz_0^S} \int_{T_l}^{T} \Theta^+(T)\,\zeta_0(T) \frac{dz_0^S}{dT}\,dT\right]\right\} \quad \text{for} \quad T \in \mathscr{S}_0. \tag{57}$$

The distance along the slip line is again given by (53) with α now set to zero.

8. Examples

In this section we present some examples of interpenetrating flows which were chosen to illustrate the following three more or less representative configurations: a jet penetrating a stream while attached to a downstream wall, a jet penetrating a stream with a stagnation region on its downstream side, and a jet having flowing streams on either side.

8.1. *A separated jet*

As a first application of the general procedure consider the separated jet shown in the dimensionless physical plane in figure 5 (*a*). The upstream and downstream walls are horizontal plates of infinitesimal thickness (Goldstein & Braun 1969*a*). The zeroth-order solution (no difference in total pressure between jet and stream) was essentially obtained by Ehrich (1953). The potential, hodograph and T planes are shown in figures 5 (*b*), (*c*) and (*d*), respectively, where corresponding points are designated by the same numbers as in the z plane (figure 5*a*). The zeroth-order 'slip line' is shown dashed in these figures since it does not correspond to a line of discontinuity and can, therefore, be ignored as far as obtaining the zeroth-order solution is concerned. Simple applications of the Schwarz–Christoffel and linear fractional transformations (Churchill 1960, §§ 34 and 92) show that the mappings which properly transform the zeroth-order w† and ζ planes into the upper half T plane are

$$w_0 = \pi^{-1}(T + 1 + \ln T) - i \tag{58}$$

and

$$\zeta_0 = [T - 2\Delta - 2i\Delta^{\frac{1}{2}}(T - \Delta)^{\frac{1}{2}}]/T. \tag{59}$$

† w_0 denotes the zeroth-order complex potential related to ζ_0 by $\zeta_0 = dw_0/dz$.

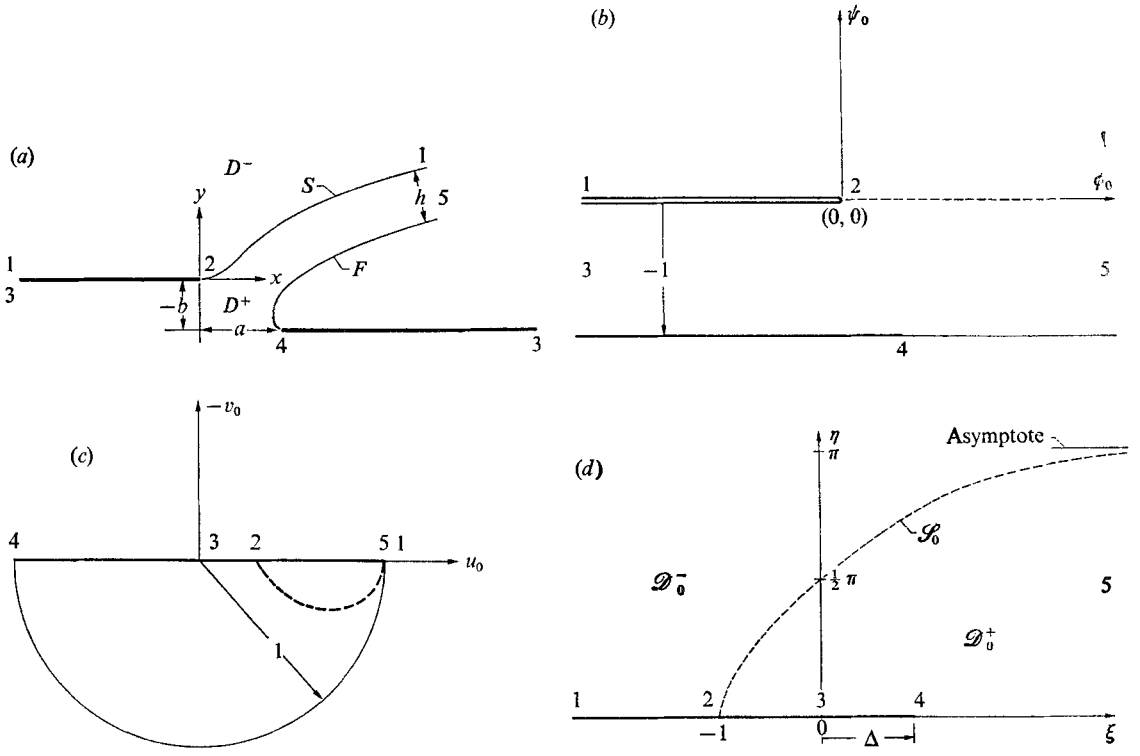

FIGURE 5. Separated jet in (*a*) physical (z) plane, (*b*) zeroth-order complex-potential (w_0) plane, (*c*) zeroth-order hodograph (ζ_0) plane and (*d*) intermediate (T) plane.

The mapping from the T plane on to the z plane is given by

$$z(T) = a + ib + \frac{1}{\pi}\left[(T-\Delta)\left(1-\frac{2}{T}\right) + 2i\Delta^{\frac{1}{2}}\left(2-\frac{1}{T}\right)(T-\Delta)^{\frac{1}{2}} - b\ln\left(\frac{i(T-\Delta)^{\frac{1}{2}}+\Delta^{\frac{1}{2}}}{\Delta^{\frac{1}{2}}}\right)\right], \tag{60}$$

where by definition $z(\Delta) = a + ib = (A + iB)/H_0$ and the dimensionless co-ordinates of the downstream lip are given by

$$a = \frac{1}{\pi}\left[3(\Delta+1) + (2\Delta-1)\ln\left(\frac{(1+\Delta)^{\frac{1}{2}}-\Delta^{\frac{1}{2}}}{\Delta^{\frac{1}{2}}}\right)^2 + 6\Delta^{\frac{1}{2}}(1+\Delta)^{\frac{1}{2}}\right]$$

and

$$b = 2(2\Delta - 1).$$

It follows from figure 5 (*b*) that the zeroth-order slip line is determined by

$$\operatorname{Im} w_0 = 0, \quad \operatorname{Re} w_0 > 0.$$

Hence, upon using (58), we find that $T \in \mathscr{S}_0$ whenever

$$T = -\eta e^{i\eta}/\sin\eta, \quad 0 < \eta < \pi. \tag{61}$$

Moreover figure 2 shows that the zeroth-order free streamline is determined by

$$T = \xi > \Delta. \tag{62}$$

By substituting (61) and (62) into (60) we can calculate, respectively, the position z_0^S of S_0 and the position z_0^F of F_0.

In order to obtain the first-order solution it is first necessary to evaluate the constants α and c_0 appearing in (45).

With no loss of generality we can choose the lower limit of the integral in (45) to be $T_l = -1$. Then, since $d\Omega_0/dz$ is infinite at $T = \Delta$, $\Omega_1^+(T)$ will be bounded at this point only if

$$\int_{-1}^{\Delta} \frac{\Theta(T)\,dT}{\zeta_0(T)} + c_0 \int_{-1}^{\Delta} \frac{dT}{\zeta_0(T)} + \alpha z(\Delta) = 0. \tag{63}$$

We can relate the constant α to the first-order thickness of the jet h_1 by equating the mass flow through the orifice to the mass flow far out in the jet. The (dimensionless) flow through the orifice is

$$Q = -\operatorname{Im} \int_{-1}^{\Delta} \zeta^+(T) \frac{dz(T)}{dT}\, dT. \tag{64a}$$

Far downstream the velocity of the jet is real and uniform, so that its magnitude may be obtained from (8) while the jet width is given by the expansion (13). Hence an alternative expression for the flow is

$$Q = (1+\epsilon)^{\frac{1}{2}}(1+\epsilon h_1 + \ldots). \tag{64b}$$

Introducing (5) and (13) into (64) and equating the two expressions for Q shows that

$$-\operatorname{Im} \int_{-1}^{\Delta} \zeta_0(T) \frac{dz(T)}{dT}\, dT = 1 \tag{65}$$

and

$$-\operatorname{Im} \int_{-1}^{\Delta} \zeta_0(T)\, \Omega_1^+(T) \frac{dz(T)}{dT}\, dT = \tfrac{1}{2} + h_1. \tag{66}$$

The first of these relations is just a result of the scaling in the zeroth-order problem. Upon introducing (64*a*), (65) and (66) into (46) (with $T_l = T_i = -1$) and recalling that $\Theta(T)$ is real on the real axis we find that

$$\alpha = -h_1. \tag{67}$$

We now return to the problem of solving (63) for α and c_0, or in view of (67), for h_1 and c_0. Substituting (59), (60) and (67) into (63) shows that

$$\int_{-1}^{\Delta} \frac{T - 2\Delta + 2i\Delta^{\frac{1}{2}}(T-\Delta)^{\frac{1}{2}}}{T}\, \Theta(T)\, dT + c_0 \left[\Delta + 1 + 2\Delta \ln \left(\frac{(1+\Delta)^{\frac{1}{2}} - \Delta^{\frac{1}{2}}}{\Delta^{\frac{1}{2}}} \right)^2 \right.$$
$$\left. + 4\Delta^{\frac{1}{2}}(1+\Delta)^{\frac{1}{2}} \right] - \frac{h_1}{\pi} \left[3(\Delta+1) + (2\Delta - 1) \ln \left(\frac{(1+\Delta)^{\frac{1}{2}} - \Delta^{\frac{1}{2}}}{\Delta^{\frac{1}{2}}} \right)^2 + 6\Delta^{\frac{1}{2}}(1+\Delta)^{\frac{1}{2}} \right]$$
$$+ 4i\pi\Delta c_0 - 2ih_1(2\Delta - 1) = 0.$$

But

$$\int_{-1}^{\Delta} \frac{T - 2\Delta + 2i\Delta^{\frac{1}{2}}(T-\Delta)^{\frac{1}{2}}}{T}\, \Theta(T)\, dT$$
$$= \int_{-1}^{\Delta} \Theta(\xi)\, d\xi - 2\Delta^{\frac{1}{2}} \int_{-1}^{\Delta} \frac{\Delta^{\frac{1}{2}} - 1 - i(T-\Delta)^{\frac{1}{2}}}{T}\, \Theta(T)\, dT.$$

In view of the singularity in the denominator, the second integral must first be carried out over the path shown in figure 6, and then the limit $\delta \to 0$ can be taken.

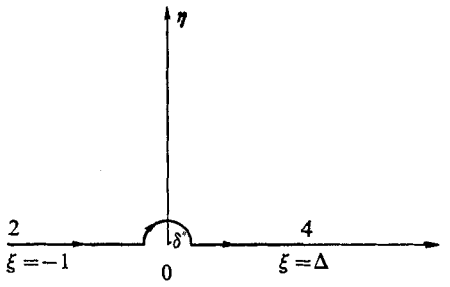

FIGURE 6. Path of integration for $\int_{-1}^{\Delta} \frac{\Delta^{\frac{1}{2}} - i(T-\Delta)^{\frac{1}{2}}}{T} \Theta(T)\, dT$ in T plane.

After performing this operation and taking the real and imaginary parts of the resulting expression we find that

$$\int_{-1}^{\Delta} \Theta(\xi)\, d\xi - 2\Delta^{\frac{1}{2}} \mathrm{P} \int_{-1}^{\Delta} \frac{\Delta^{\frac{1}{2}} + (\Delta+\xi)^{\frac{1}{2}}}{\xi} \Theta(\xi)\, d\xi + c_0[\Delta + 1 + 4\Delta^{\frac{1}{2}}(1+\Delta)^{\frac{1}{2}}]$$
$$- \frac{3h_1}{\pi}[\Delta + 1 + 2\Delta^{\frac{1}{2}}(1+\Delta)^{\frac{1}{2}}] + \left[c_0 2\Delta - \frac{h_1}{\pi}(2\Delta - 1)\right] \ln\left(\frac{(1+\Delta)^{\frac{1}{2}} - \Delta^{\frac{1}{2}}}{\Delta^{\frac{1}{2}}}\right)^2 = 0$$

and
$$2\pi\Delta c_0 - h_1(2\Delta - 1) + 2\pi\Delta\Theta(0) = 0.$$

Finally, upon eliminating c_0 between these two equations we find that

$$h_1 = \frac{-2\pi\Delta}{(\Delta+1)[4\Delta + 1 + 4\Delta^{\frac{1}{2}}(\Delta+1)^{\frac{1}{2}}]} \left\{ 2\Delta^{\frac{1}{2}} \mathrm{P} \int_{-1}^{\Delta} \frac{\Delta^{\frac{1}{2}} + (\Delta-\xi)^{\frac{1}{2}}}{\xi} \Theta(\xi)\, d\xi \right.$$
$$\left. - \int_{-1}^{\Delta} \Theta(\xi)\, d\xi + \left[\Delta + 1 + 2\Delta \ln\left(\frac{(1+\Delta)^{\frac{1}{2}} - \Delta^{\frac{1}{2}}}{\Delta^{\frac{1}{2}}}\right)^2 + 4\Delta^{\frac{1}{2}}(1+\Delta)^{\frac{1}{2}}\right] \Theta(0) \right\} \quad (68)$$

and
$$c_0 = \frac{(2\Delta - 1)}{2\pi\Delta} h_1 - \Theta(0). \quad (69)$$

With the constants α and c_0 now determined by (67)–(69) it is possible to calculate Ω_1^+ by quadrature from (38), (40), (41), (45), (59) and (61) and hence to obtain the slip-line position from (48) and (59)–(61) and the free-streamline position from (49), (59), (60) and (62). If T is on $\mathscr{S}_0 + \mathscr{S}_0'$ equation (42) with the plus sign (since T approaches the contour from within $\mathscr{S}_0^+$) must be used in place of (41) to calculate $\Theta(T)$. The pressure coefficient and distance along the slip line are given by (51) and (53).

The shapes of the jet boundaries for various values of the parameters ϵ and B/A are shown in figures 7–9. As the total pressure in the jet increases above the ambient value, the volume occupied by the jet increases. This is due to the fact that the uppermost streamline rises more than the lowermost. This effect is most evident in figure 7, which corresponds to a jet injected normal to the mainstream ($B = 0$). When the orifice angle $\tan^{-1} B/A$ is greater than or equal to zero, a small change in the total pressure within the jet results in a large change in both the jet penetration and jet thickness. This effect becomes more pronounced as the orifice angle is increased. In fact, it becomes so pronounced that it is felt that the analysis may not be valid for orifice angles larger than 45°. Figure 8 shows that,

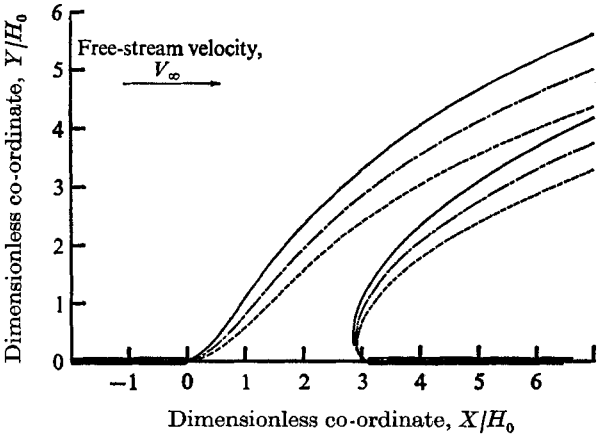

FIGURE 7. Separated-jet contour for an orifice offset ratio $B/A = 0$.
– – –, $\epsilon = 0$; —·—, $\epsilon = 0{\cdot}1$; ——, $\epsilon = 0{\cdot}2$.

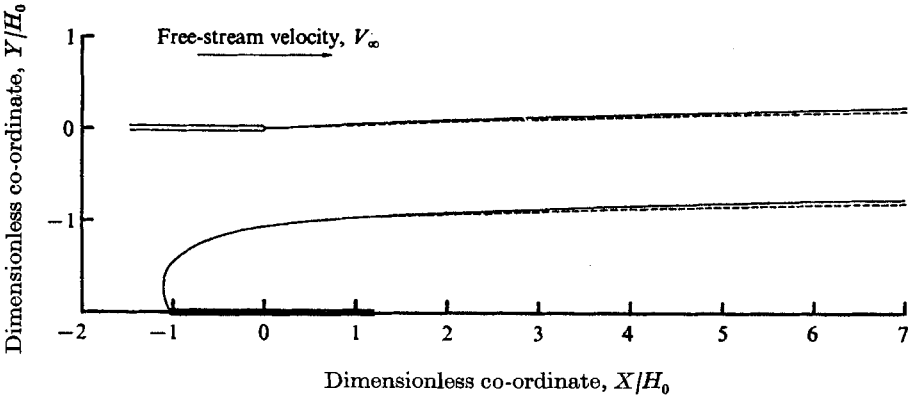

FIGURE 8. Separated-jet contour for an orifice offset ratio $B/A = -2$.
– – –, $\epsilon = 0$; ——, $\epsilon = 0{\cdot}3$.

for sufficiently large negative values of the orifice angle, changes in the total pressure within the jet have almost no effect on the jet penetration or on the jet thickness. Although the scale of the figures is too small to show this, the numerical results do show that the jet always leaves the wall in a tangential direction.

The ratio of the jet width at large distances downstream to the distance from lip to lip across the orifice is defined as the contraction ratio. Its variation with orifice angle is shown in figure 10. It is apparent that turning the jet into the mainstream tends markedly to decrease the contraction ratio, signifying that there is a decrease in the flow within the jet. The indications are, however, that a slight increase in the total pressure in the jet can easily compensate for this decreased flow. The jet penetration also increases with increasing orifice angle.

The slip-line pressure coefficient is shown in figures 11 (*a*)–(*d*). Each figure is for a different orifice angle. These curves contain all the information necessary for calculating the viscous boundary layer along the slip line. They show that the velocity within the jet at the upstream edge of the orifice decreases with both

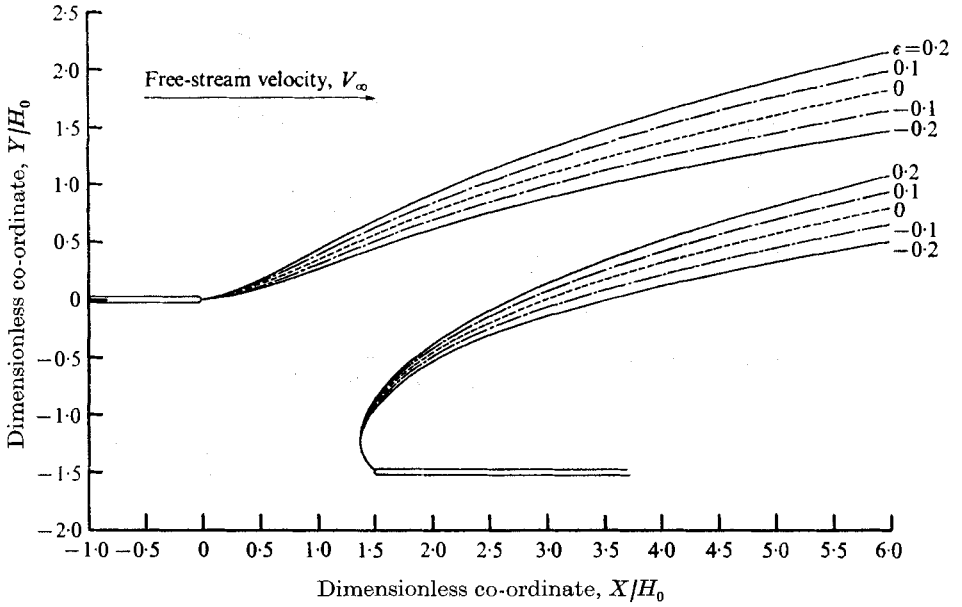

FIGURE 9. Separated-jet contour for an orifice offset ratio $B/A = -1$.

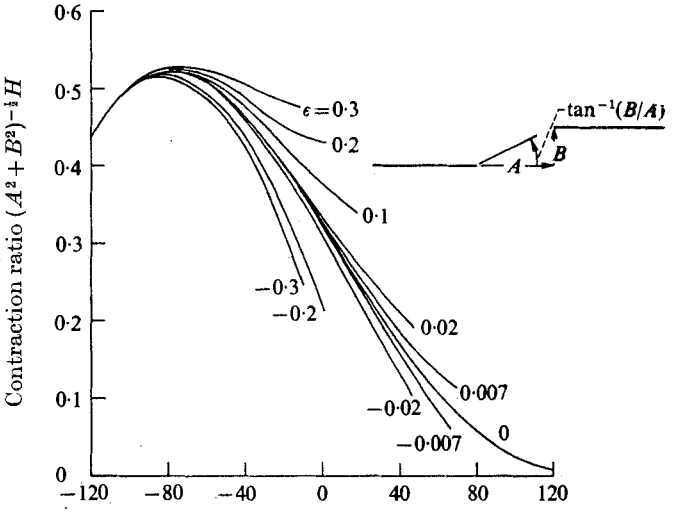

FIGURE 10. Jet contraction ratio for a separated jet.

increasing orifice angle and decreasing ϵ. It can also be seen from these curves that the pressure coefficient nearly achieves its asymptotic value in a distance of 10 jet diameters downstream.

8.2. *An attached jet*

As a second example consider a jet attached to the downstream wall (Goldstein & Braun 1969*b*). The (dimensionless) z plane is shown in figure 12 (*a*). The zeroth-order T plane is the same as that shown in figure 5 (*d*) and the zeroth-order

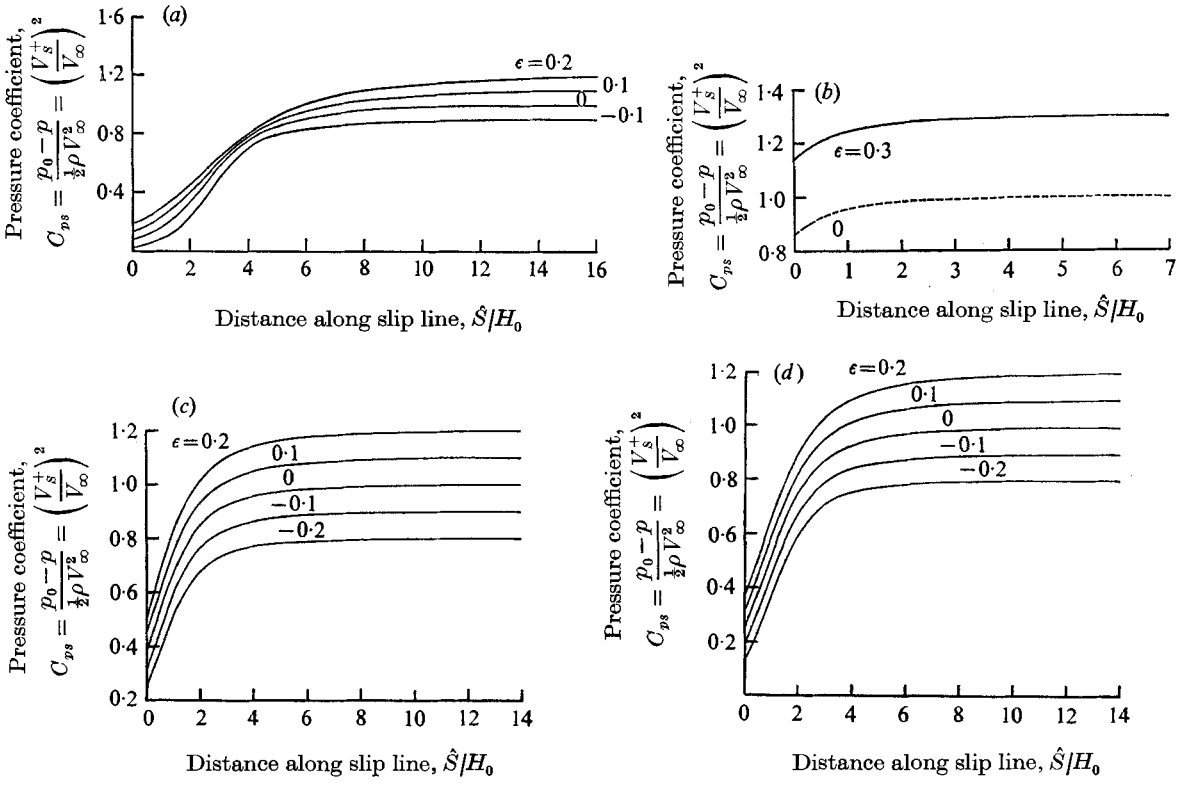

FIGURE 11. Pressure coefficients on slip line of separated jet for various orifice offset ratios. (*a*) $B/A = 0$. (*b*) $B/A = 2$ (third quadrant). (*c*) $B/A = -2$ (fourth quadrant). (*d*) $B/A = -1$ (fourth quadrant).

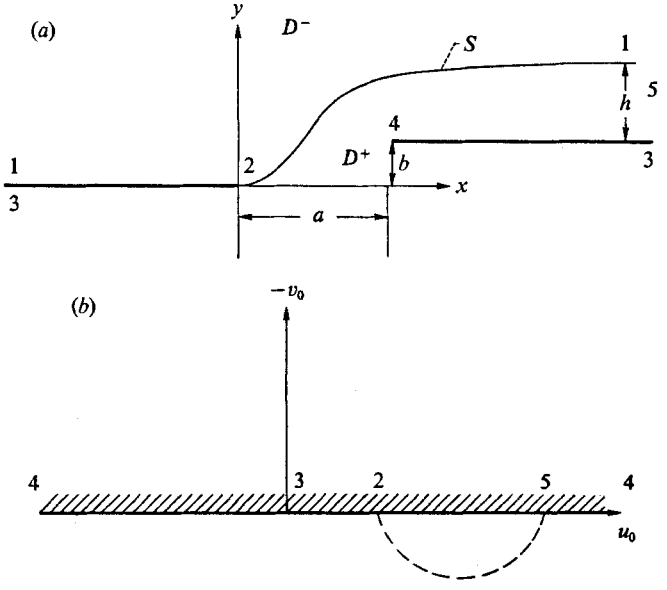

FIGURE 12. (*a*) Physical (z) plane and (*b*) zeroth-order hodograph (ζ_0) plane for an attached jet.

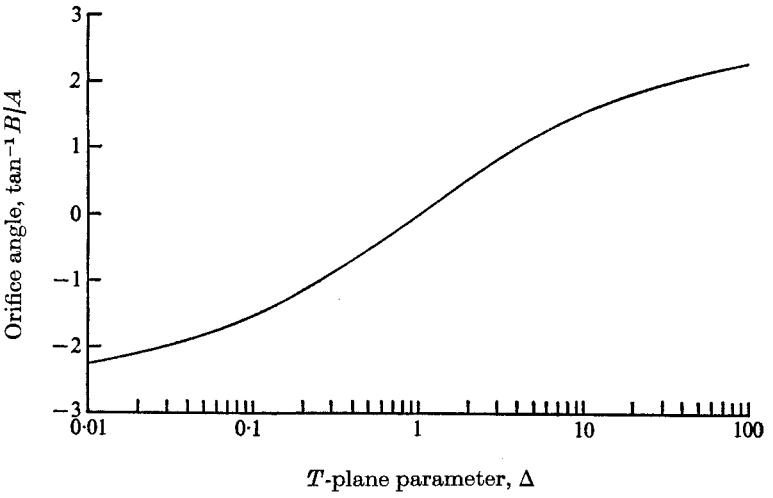

FIGURE 13. Dependence of orifice angle on the parameter Δ.

hodograph plane is shown in figure 12 (*b*). The zeroth-order potential plane and hodograph plane are transformed to the T plane by (58) and by

$$\zeta_0 = T/(T-\Delta), \quad \eta \geqslant 0. \tag{70}$$

The physical plane is mapped into the T plane by

$$z(T) = \frac{1}{\pi}\left[T + (1-\Delta)\ln\frac{T}{\Delta} + \frac{\Delta}{T} - (1+\Delta)\right] + a + ib, \tag{71}$$

where, by definition,

$$\begin{aligned} z(\Delta) &= (A+iB)/H_0 = a+ib \\ &= \pi^{-1}[(1-\Delta)\ln\Delta + 2(1+\Delta)] + i(\Delta-1). \end{aligned}$$

As in the previous example $\mathscr{S}_0$ (the zeroth-order slip line in the T plane) is determined by (61). The function Θ can now be calculated by substituting (40), (55), (61) and (70) into (41) [or (42) if T is on $\mathscr{S}_0$] and carrying out the integration. The slip-line position and pressure coefficient can then be obtained by substituting this expression along with (70) into (56) and (57), respectively, and carrying out the quadratures. The distance along the slip line is obtained in a similar way from (53).

The asymptotic jet thickness can be found by equating the mass flow through the orifice [calculated from (64 *a*)] to the mass flow far downsteam in the jet [calculated from (64 *b*)] to obtain $h_1 = \Theta^+(0)$. Then upon using the results of this section to evaluate $\Theta^+(0)$ we find that

$$h = 1 + \epsilon h_1 = 1 + \frac{\mathrm{Si}\,(2\pi)}{2\pi}\epsilon\Delta\left(1+\frac{\Delta}{2}\right) = 1 + 0{\cdot}4514\epsilon\Delta\left(1+\frac{\Delta}{2}\right),$$

where Si is the sine integral. The parameter Δ is related to the orifice angle in the manner shown in figure 13.

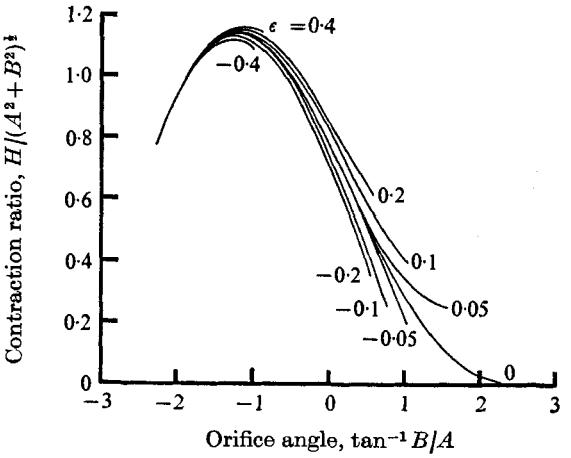

FIGURE 14. Jet contraction ratio.

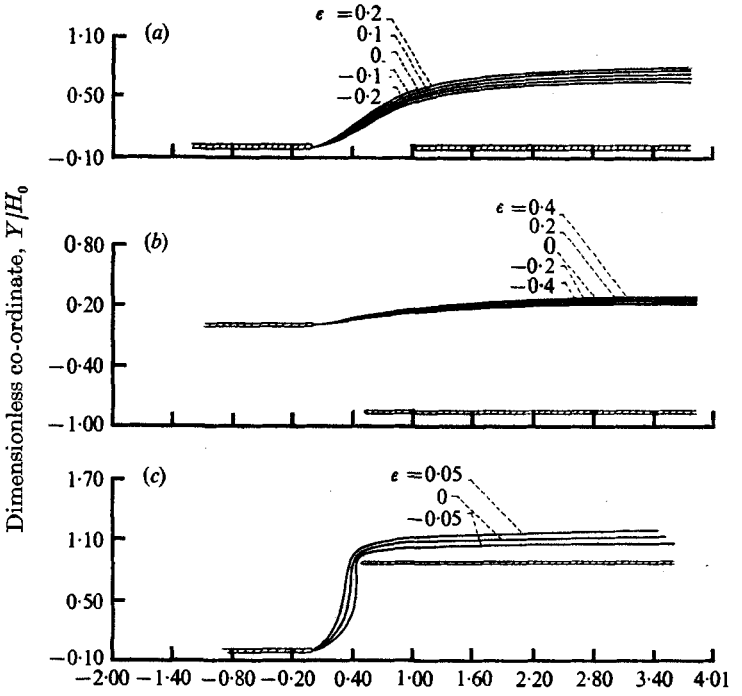

FIGURE 15. Attached-jet contours for various orifice offset ratios and values of ϵ.
(*a*) $B/A = 0$. (*b*) $B/A = -3^{\frac{1}{2}}$. (*c*) $B/A = 3^{\frac{1}{2}}$.

The jet contraction ratio $h/(a^2+b^2)^{\frac{1}{2}}$ is plotted in figure 14 and the shapes of the jet boundaries for various values of the parameters ϵ and B/A are shown in figure 15. Figure 15 (*a*) corresponds to a jet injected normal to the mainstream ($B = 0$), figure 15 (*b*) to negative orifice angles (i.e. jets injected downstream) and figure 15 (*c*) to positive orifice angles (i.e. jets injected upstream). The

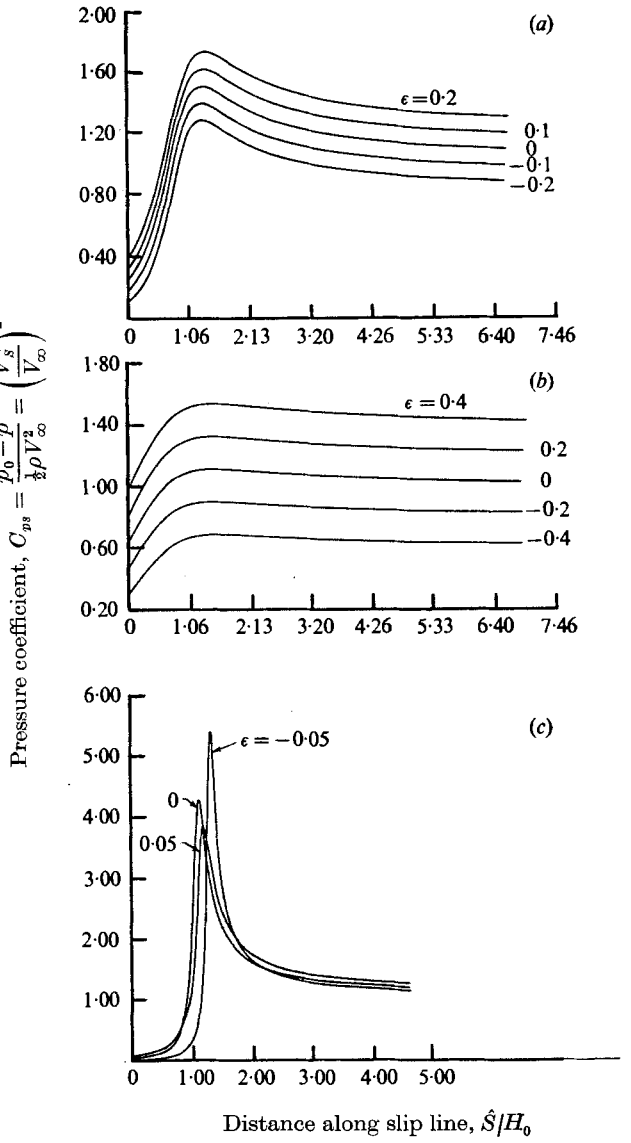

FIGURE 16. Pressure coefficients on slip line of attached jet for various orifice offset ratios and values of ϵ. (*a*) $B/A = 0$. (*b*) $B/A = -3^{\frac{1}{2}}$ (fourth quadrant). (*c*) $B/A = 3^{\frac{1}{2}}$ (first quadrant).

configuration shown in figure 15 (*c*) may be strongly modified by viscous effects. Figures 15 (*a*) and (*c*) show that small changes in the jet's total pressure result in quite large changes in both the jet penetration and jet thickness, whenever the orifice angle is greater than zero. This effect becomes more pronounced as the orifice angle is increased.

The numerical results show that the rate of change of the jet penetration distance with the total-pressure difference ϵ can be approximated by an exponential function of the form $ae^{b\nu}$, where ν is the orifice angle $\tan^{-1} B/A$. This

relation holds for both the separated and attached jets. At $X = 3{\cdot}4H_0$, b is approximately 1·5 for both types of jet. This shows that in both cases the sensitivity of the penetration distance to the dimensionless total pressure difference ϵ is a very strong function of the orifice angle. The figures also show that turning the jet into the mainstream tends markedly to decrease the flow in the jet. The extreme sensitivity of the flow configuration to ϵ at large positive orifice angles indicates that the perturbation analysis will eventually break down when the orifice angle gets large enough.

The results of the pressure-coefficient calculations are shown in figure 16. Each figure is for a different orifice angle. These curves contain all the information necessary for calculating the viscous boundary layer along the slip line. They show that the velocity at both the upstream edge of the orifice and at the downstream end of the slip line increases with increasing ϵ provided that the orifice angle remains constant. For negative orifice angles the velocity tends to be relatively constant along the slip line, exhibiting a slight dip at the upstream edge of the orifice. As the orifice angle is increased towards zero the variation of the velocity along the slip line becomes more pronounced. For non-negative values of the orifice angle there is a definite peak in the velocity profiles which becomes more marked as the angle is increased. We attribute this to the fact that the velocity is infinite at the downstream edge of the orifice. Since this point moves closer to the slip line as the orifice angle is increased, it is natural that the velocity along the slip line should become more peaked with increasing orifice angle.

8.3. *A jet injected between two streams*

There are various situations of technological interest where a stream of fluid is injected into the midst of a moving flow. This occurs, for example, when water discharges into a river, when gas is blown from an exhaust into the wind or when gaseous fuel is injected into a stream of oxidant. The dimensionless physical plane for such a configuration is shown in figure 17 (*a*) (Goldstein & Siegel 1972). The injected flow can turn and either contract or expand as it meets the mainstream. Since this example is similar to the preceding one we shall merely indicate the results.

The intermediate T plane is chosen in the manner indicated in figure 17 (*b*), the curves $\mathscr{S}_0^{(\mathrm{I})}$ and $\mathscr{S}_0^{(\mathrm{II})}$ being the images of the zeroth-order slip lines $S_0^{(\mathrm{I})}$ and $S_0^{(\mathrm{II})}$ respectively.

The mapping of the zeroth-order hodograph plane into the upper half T plane is

$$\zeta_0 = \left(\frac{T+\gamma}{T+1}\right)^{\lambda} \quad \text{for} \quad \eta \geqslant 0; \quad \delta = 1/\gamma^2,$$

where $\pi\lambda$ is the deflexion angle of the flap and $\delta \equiv \Delta/H_0$ is the ratio of the nozzle width to the zeroth-order asymptotic jet width. The points in the physical plane are related to the points in the T plane by

$$z(T) = -\frac{1}{\pi\gamma_3\gamma_6}\int_{-1}^{T}\left(\frac{T+1}{T+\gamma}\right)^{\lambda}\frac{(T+\gamma_3)(T-\gamma_6)}{T}\,dT,$$

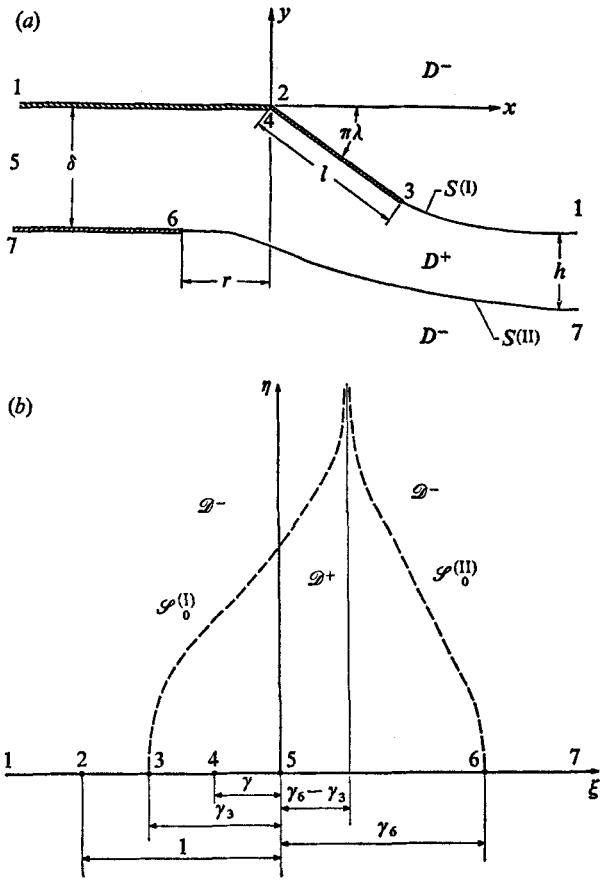

FIGURE 17. (*a*) Flow geometry and nomenclature and (*b*) intermediate (T) plane (shown for $\gamma_6 > \gamma_3$) for a jet between two moving streams.

where $\gamma_3 = (\beta_3+\gamma)/(\beta_3+1)$ and $\gamma_6 = (\beta_6-\gamma)/(1-\beta_6)$ while β_3, β_6 and γ are related to the dimensionless lengths $l = L/H_0$ and $r = R/H_0$ (shown in figure 17*a*) by

$$(\gamma-\beta_6)(\gamma+\beta_3)[1-\delta-\lambda(\gamma-1)] = \tfrac{1}{2}\lambda(\lambda+1)(\gamma-1)^2(\beta_3+1)(\beta_6-1)-\lambda(\gamma-1)^3,$$

$$r = \frac{(1-\gamma)^3}{\pi(\beta_3+\gamma)(\beta_6-\gamma)}\,\mathrm{P}\int_0^{\beta_6}\frac{1}{\sigma^\lambda}\frac{(\beta_3+\sigma)(\sigma-\beta_6)}{(\sigma-\gamma)(1-\sigma)^3}\,d\sigma$$

and

$$l = \frac{(1-\gamma)^3}{\pi(\beta_3+\gamma)(\beta_6-\gamma)}\int_0^{\beta_3}\frac{1}{\sigma^\lambda}\frac{(\beta_3-\sigma)(\sigma+\beta_6)}{(\sigma+1)^3(\sigma+\gamma)}\,d\sigma.$$

The curves $\mathscr{S}_0^{(\mathrm{I})}$ and $\mathscr{S}_0^{(\mathrm{II})}$ (appropriately extended into the lower half-plane) are given parametrically by†

$$T = \left.\begin{cases} T^{(1)}(\omega) & \text{with} \quad -\omega_m \leqslant \omega \leqslant \omega_m \\ T^{(2)}(\omega) & \text{with} \quad \omega_m \geqslant \omega > \tfrac{1}{2}\pi, \quad -\tfrac{1}{2}\pi > \omega \geqslant -\omega_m \\ T^{(2)}(\omega) & \text{with} \quad -\tfrac{1}{2}\pi < \omega < \tfrac{1}{2}\pi \quad \text{for} \quad T \in \mathscr{S}_0^{(\mathrm{II})} \end{cases}\right\} \quad \text{for} \quad T \in \mathscr{S}_0^{(\mathrm{I})} \Bigg\} \quad \text{for} \quad \gamma_6 > \gamma_3$$

† The curves are traversed in a positive (clockwise) direction as ω changes from the left- to the right-hand limit in the inequalities.

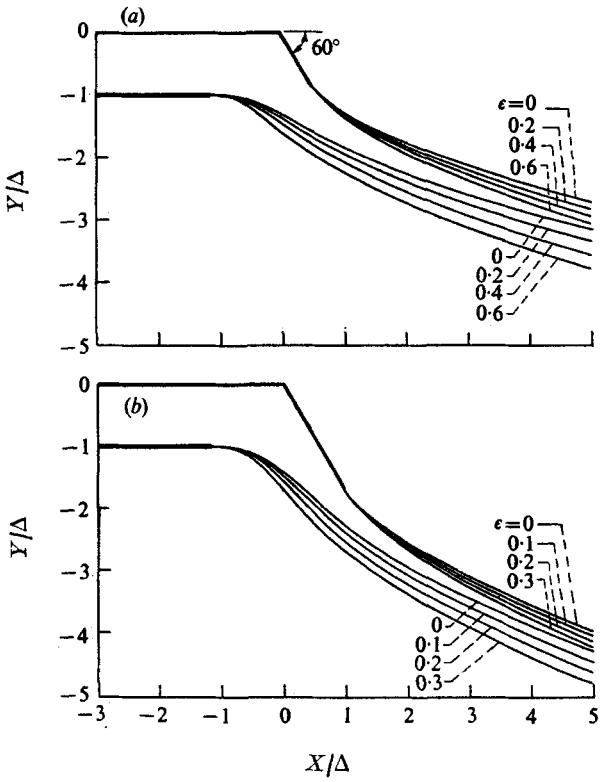

FIGURE 18. Jet slip-line boundaries for outlet with 60° plate deflexion angle; $R/\Delta = 1$. (*a*) $L/\Delta = 1$. (*b*) $L/\Delta = 2$.

and

$$T = \left\{ \begin{matrix} T^{(1)}(\omega) & \text{with} & -\tfrac{1}{2}\pi < \omega < \tfrac{1}{2}\pi & \text{for} & T \in \mathscr{S}_0^{(\mathrm{I})} \\ T^{(2)}(\omega) & \text{with} & -\omega_m \leqslant \omega \leqslant \omega_m & & \\ T^{(1)}(\omega) & \text{with} & \omega_m \geqslant \omega > \tfrac{1}{2}\pi, & -\tfrac{1}{2}\pi > \omega \geqslant -\omega_m & \end{matrix} \right\} \text{ for } T \in \mathscr{S}_0^{(\mathrm{II})} \Bigg\} \text{ for } \gamma_6 < \gamma_3,$$

where $T^{(k)}(\omega) \equiv \frac{1}{2}[\gamma_6 - \gamma_3 + (-1)^k((\gamma_6-\gamma_3)^2 + 4\gamma_3\gamma_6\omega\cot\omega)^{\frac{1}{2}}](1 + i\tan\omega)$ and ω_m is the solution of the transcendental equation $(\gamma_6-\gamma_3)^2\tan\omega_m + 4\gamma_3\gamma_6\omega_m = 0$ for $\omega_m \geqslant 0$. The physical location of the slip lines $S^{(\mathrm{I})}$ and $S^{(\mathrm{II})}$ can now be calculated by using these results in (40), (41), (55) and (56) in the manner indicated in §8.2

Figure 18 shows the slip lines for positive values of the angle $\pi\lambda$ and various values of the total-pressure difference parameter ϵ. As ϵ is increased, the total pressure in the jet increases above that in the stream. This produces two effects on the slip-line configuration: first the jet width expands; and second the jet deflexion tends to persist over a longer path, that is, it is more difficult for the outer stream to turn the jet into the horizontal direction.

Results for negative λ are shown in figure 19. Their validity depends upon the flow remaining attached to the upper boundary by means of the Coanda effect – which can be promoted by boundary-layer control. The contraction ratio H_0/Δ is

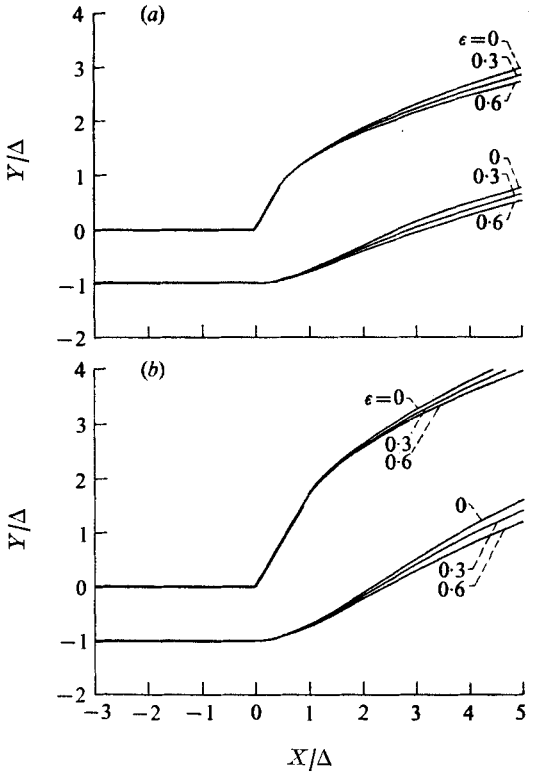

FIGURE 19. Jet slip-line boundaries for zero orifice offset distance ($R/\Delta = 0$) and a plate deflexion angle of $-60°$. (*a*) $L/\Delta = 1$. (*b*) $L/\Delta = 2$.

larger than unity in this instance as the flap is expanding the jet by virtue of the attachment of the upper jet streamline. When ϵ is increased, the width of the jet tends to expand and its path becomes more horizontal.

9. Conclusions

The theory of sectionally analytic functions provides a method for extending the classical analysis of inviscid interpenetrating streams to situations where there is a small difference in total pressure. Calculations of specific examples show that the sensitivity of the jet width and penetration to the pressure difference is strongly dependent upon the angle at which the orifice or nozzle is positioned.

The authors are indebted to Miss Jean Healy for carrying out the numerical computations. Some of the results in this paper were given in a preliminary form in several N.A.S.A. reports (Goldstein & Braun 1969*a*, *b*; Goldstein & Siegel 1972).

Appendix

Let δ denote any streamline whose zeroth-order position is δ_0. Then we can put the points z^δ on δ into one-to-one correspondence with the points z_0^δ of δ_0 in such a way that $z^\delta - z_0^\delta = O(\epsilon)$ using the relation

$$\mathrm{Re}\{\zeta^+(z^\delta)\,dz^\delta\} = [1+\epsilon f(\delta_0)]\,\mathrm{Re}\{\zeta_0(z_0^\delta)\,dz_0^\delta\}, \tag{A 1}$$

where $f(\delta_0)$ is an arbitrary, monotonically increasing, real function of the arc length δ_0.

The condition that the velocity and arc element are parallel, both on the streamline δ and the zeroth-order streamline δ_0, is

$$\mathrm{Im}\{\zeta^+(z^\delta)\,dz^\delta\} = \mathrm{Im}\{\zeta_0(z_0^\delta)\,dz_0^\delta\} = 0. \tag{A 2}$$

The sum of (A 1) and (A 2) yields

$$\zeta^+(z^\delta)\,dz^\delta = [1+f(\delta_0)]\,\zeta_0(z_0^\delta)\,dz_0^\delta. \tag{A 3}$$

On the left side of (A 3) we introduce an expansion of the type (17) or (18) as well as the expansion $dz^\delta = dz_0^\delta + \epsilon dz_1^\delta$ to show that

$$[\partial(\zeta_0 z_1^\delta)/\partial z_0^\delta]_{z_0^\delta} = \zeta_0(z_0^\delta)\,[f(\delta_0) - \Omega_1^+(z_0^\delta)].$$

Integration from a point $z = z_0^i$ at which $z_1^\delta = 0$ yields

$$z^\delta = z_0^\delta + \epsilon z_1^\delta = z_0^\delta + \frac{\epsilon}{\zeta_0(z_0^\delta)} \int_{z_0^i}^{z_0^\delta} \zeta_0(z_0^\delta)\,[f(\delta_0) - \Omega_1^+(z_0^\delta)]\,dz_0^\delta. \tag{A 4}$$

REFERENCES

Ackerberg, R. C. & Pal, A. 1968 On the interaction of a two-dimensional jet with a parallel flow. *J. Math. Phys.* **47**, 32.

Birkhoff, G. & Zarantonello, E. H. 1957 *Jets, Wakes, and Cavities.* Academic.

Churchill, R. V. 1960 *Complex Variables and Applications.* McGraw-Hill.

Ehrich, F. F. 1953 Penetration and deflection of jets oblique to a general stream. *J. Aero. Sci.* **20**, 99.

Gakhov, F. D. 1966 *Boundary Value Problems* (trans. I. N. Sneddon). Oxford: Pergamon.

Goldstein, M. E. & Braun, W. 1969*a* Injection of an inviscid separated jet at an oblique angle to a moving stream. *N.A.S.A. Tech. Note*, D-5460.

Goldstein, M. E. & Braun, W. 1969*b* Injection of an attached inviscid jet at an oblique angle to a moving stream. *N.A.S.A. Tech. Note*, D-5501.

Goldstein, M. E. & Siegel, R. 1972 Inviscid analysis of jet injection between two moving streams. *N.A.S.A. Tech. Note*, D-6780.

Muskhelishvili, N. I. 1953 *Singular Integral Equations* (trans. J. R. M. Radok). Groningen: P. Noordhoff.

Spence, D. A. 1956 The list of a thin jet-flapped wing. *Proc. Roy. Soc.* A **238**, 46.

Taylor, G. I. 1954 The use of a vertical air jet as a windscreen. *Mémoires sur la Mécanique des Fluides., Publ. Sci. Tech. Ministère de l'Air, Paris*, no. 313.

Woods, L. C. 1956 *Quart. J. Mech. Appl. Math.* **9**, 441.